CREEP OF METAL-MATRIX COMPOSITES WITH ELASTIC FIBERS—PART II: A DAMAGE MODEL

CAO CHENG and N. ARAVAS

Department of Mechanical Engineering and Applied Mechanics, University of Pennsylvania, Philadelphia, PA 19104, U.S.A.

Abstract—A constitutive model that accounts for the effects of fiber failure on the high temperature mechanical behavior of metal-matrix composites (MMC) reinforced by long brittle fibers is presented. Weibull statistics are used to describe the strength of the fibers and the assumption of 'global load sharing' is used to determine the average stress in the fibers. The developed three-dimensional constitutive model involves a 'damage parameter' that accounts for the accumulated fiber failure. A method for the numerical integration of the constitutive equations is developed. The proposed model is used together with the finite element method to predict the life of a plate with a hole loaded in tension in the direction of the fibers under creep conditions. © 1997 Elsevier Science Ltd.

1. INTRODUCTION

A constitutive model for the mechanical behavior of metal-matrix composites reinforced by elastic fibers was presented in Part I. In developing that model, we assumed that the fibers remain intact as the composite deforms. However, it has been established that fibers in many composites experience strength degradation during deformation (Prewo, 1986; Thouless *et al.*, 1989). The effects of fiber failure on the creep behavior of metal-matrix composites are examined in detail in the present paper.

The material systems considered are the same as those of Part I. The response of the composite to shear loads relative to the fibers will be matrix-dominated, and fiber failure is not expected to affect significantly the performance of the composite under such loads. On the other hand, when axisymmetric loads are applied, fiber failure plays a very important role and can lead eventually to failure of the composite.

When a composite specimen is subjected to a uniaxial stress in the direction of the fibers, load is continuously transferred from the matrix to the fibers. When the applied stress is held constant and if the fibers remain intact, the corresponding axial strain rate decreases since the matrix stress relaxes due to matrix creep; as time progresses, the matrix is completely unloaded, the whole load is carried by the fibers, and the strain rate vanishes eventually. However, when fibers break, the fibers are locally unloaded, load is transferred back to the matrix, and the strain rate increases; this can cause, in turn, more fibers to break, and can lead eventually to failure of the composite component. A simple model that accounts for fiber breakage in a uniaxial tension test has been presented by McLean (1989). Theoretical studies on fiber failure stochastics within the framework of 'global load sharing', whereby the load shed from a broken fiber is shared nearly equally among all intact fibers, have been carried out by Curtin (1991) for composites with weak interfaces. More recently, Du and McMeeking (1995) made use of Curtin's results and studied in detail the effects of fiber breaks and the consequential stress relaxation in the broken fibers.

In this paper we study in detail the effects of fiber failure on the high temperature mechanical behavior of metal-matrix composites. In a way similar to that of Part I, a *three dimensional* constitutive model for the composite is developed in two steps: (i) one in which shear loads relative to the fibers are applied, and (ii) another in which the composite is subjected to axisymmetric loads relative to the fibers. For the case of the shear loads, it is assumed that equations (16)-(19) of Part I that describe the behavior of the composite under shear loads, are valid, even when the fibers fail. When axisymmetric loads are applied

to the composite, Curtin's (1991) methodology is used to account for fiber failure. In fiber-reinforced metal-matrix composites, a weak fiber-matrix bond has been found to be essential to ensure good longitudinal strength (Jansson *et al.*, 1991). When a fiber breaks, the low shear strength of the interface diminishes any local stress concentrations, thus justifying the assumption of 'global load shearing'. The developed constitutive model involves a 'damage parameter' ω which takes values in the range $0 \leqslant \omega \leqslant 1$ and accounts for fiber failure. When $\omega = 0$, there is no fiber failure and the model reduces to that of Part I. Values of ω greater than zero account for the fact that, as fibers fail, the average stress in the unbroken fibers decreases, which in turn increases the stress carried by the matrix and the corresponding creep strain rate. The limiting value $\omega = 1$ corresponds to the case where the local load-carrying capacity of the composite is reduced to zero and the corresponding strain rate becomes infinite. In deriving the model, we assumed that the fiber-matrix sliding stress is constant and ignored the effects of fiber relaxation near fiber breaks. A method for the numerical integration of the proposed model is presented and the developed constitutive equations are implemented in a general-purpose finite element program. The proposed constitutive equations are used together with the finite element method to study the evolution of damage in a plate with a hole loaded in tension in the direction of the fibers under creep conditions.

Standard notation identical to that of Part I is used in the present paper.

2. THE FIBER DOMINATED BEHAVIOR FOR AXISYMMETRIC LOADING WITH DAMAGE

2.1. *McLean's model for uniaxial tension with damage*

In Section 4.1 of Part I, we gave a detailed presentation of McLean's model for the case where the fibers remain *intact* while the composite deforms. For the case of uniaxial tension, McLean assumes that the axial strain in the matrix and the fibers equals the macroscopic axial strain ε, and that uniform stresses develop in the fibers and the matrix with the only non-zero components being $\sigma_{f33} = \sigma_f^{un}$ and $\sigma_{m33} = \sigma_m$. In the absence of any fiber failure, we have that

$$\sigma = f\sigma_f^{un} + (1-f)\sigma_m \quad \text{and} \quad \dot{\varepsilon} = \frac{\dot{\sigma}_f^{un}}{E_f} = \frac{\dot{\sigma}_m}{E_m} + B\sigma_m^n, \tag{1}$$

where $\sigma_f^{un} = E_f\varepsilon$ is the stress in the unbroken fibers.

Curtin (1991) and Du and McMeeking (1995) used Weibull statistics to describe the strength of the fibers and carried out theoretical studies of fiber failure stochastics within the framework of global load sharing, for composites with weak interfaces. When the applied load in the direction of the fibers is such that the corresponding axial strain increases monotonically with time (i.e., no load reversals), they concluded that the average fiber stress $\bar{\sigma}_f$ is a nonlinear function of the macroscopic strain ε:

$$\bar{\sigma}_f = \left[1 - \frac{1}{2}\left(\frac{E_f\varepsilon}{S_c}\right)^{m+1}\right]E_f\varepsilon, \quad \text{where } S_c = \left(\frac{2S_0^m\tau_0 L_0}{D}\right)^{1/(m-1)}, \tag{2}$$

S_0 and L_0 are strength and length parameters of the Weibull distribution, m is the Weibull modulus, and τ_0 is the frictional sliding resistance between the fibers and the matrix. The derivation of eqn (2a) can be found in Du and McMeeking (1995) (see their equation (10) on page 706) and will not be repeated here. Note that, if fiber failure is ignored, then

$$\bar{\sigma}_f = E_f\varepsilon. \tag{3}$$

Equations (2a) and (3) make it clear that fiber failure reduces the stress carried by the fibers. The second term in the square brackets of eqn (2a) can be viewed as a measure of

the 'damage' in the composite; in fact, eqn (2a) can be obtained from (3) if the elastic modulus E_f of the fibers is replaced by the secant modulus E_f^{sec}, i.e.,

$$\bar{\sigma}_f = E_f^{sec}\varepsilon, \quad \text{where } E_f^{sec} = \left[1 - \frac{1}{2}\left(\frac{E_f\varepsilon}{S_c}\right)^{m+1}\right]E_f. \tag{4}$$

Using eqn (2a) we can define the corresponding tangent modulus as

$$E_f^{tan} \equiv \frac{d\bar{\sigma}_f}{d\varepsilon} = \left[1 - \frac{m+2}{2}\left(\frac{E_f\varepsilon}{S_c}\right)^{m+1}\right]E_f. \tag{5}$$

Summarizing, we mention that, for the case of uniaxial tension with monotonically increasing ε, eqns (1a, b) are replaced by

$$\sigma = f\bar{\sigma}_f + (1-f)\sigma_m \quad \text{and} \quad \dot{\varepsilon} = \frac{\dot{\bar{\sigma}}_f}{E_f^{tan}} = \frac{\dot{\sigma}_m}{E_m} + B\sigma_m^n, \tag{6}$$

when fiber failure is taken into account.

Using the last two equations we can readily show that

$$\dot{\varepsilon} = \frac{1}{1-\omega}\left[\frac{\dot{\sigma}}{E} + B'(\sigma-\alpha)^n\right] \quad \text{and} \quad \frac{\dot{\alpha}}{fE_f^{tan}} = \frac{1}{1-\omega}\left[\frac{\dot{\sigma}}{E} + B'(\sigma-\alpha)^n\right], \tag{7}$$

where ω is a 'damage parameter' defined as

$$\omega(\varepsilon) = (m+2)\frac{fE_f}{2E}\left(\frac{E_f\varepsilon}{S_c}\right)^{m+1}, \tag{8}$$

the back stress α is defined as the part of the stress carried by the fibers, i.e., $\alpha = f\bar{\sigma}_f$, $E = fE_f + (1-f)E_m$, and $B' = BE_m/[(1-f)^{n-1}E]$. The damage parameter ω is proportional to the second term in the square brackets of eqn (2a) and has been normalized in such a way that the strain rate $\dot{\varepsilon}$ approaches infinity as $\omega \to 1$. When $\omega = 0$ (intact fibers), eqns (7a, b) reduce to equations (24a, b) of Part I. A discussion of the physical meaning of ω is given in the Appendix.

The instantaneous response of the composite is elastic and the corresponding values of the strain, the back stress, and the damage parameter immediately after the application of the load are:

$$\varepsilon_0 = \sigma(0^-)/E_0, \quad \alpha_0 = fE_{f0}^{sec}\varepsilon_0, \quad \text{and} \quad \omega_0 = (m+2)\frac{fE_f}{2E}\left(\frac{E_f\varepsilon_0}{S_c}\right)^{m+1}, \tag{9}$$

where

$$E_0 = fE_{f0}^{sec} + (1-f)E_m \quad \text{and} \quad E_{f0}^{sec} = \left[1 - \frac{1}{2}\left(\frac{E_f\varepsilon_0}{S_c}\right)^{m+1}\right]E_f. \tag{10}$$

Note that eqn (9a) is a nonlinear equation that defines ε_0. When the corresponding values of ω_0 is greater than one, then the composite fails instantaneously (see Appendix).
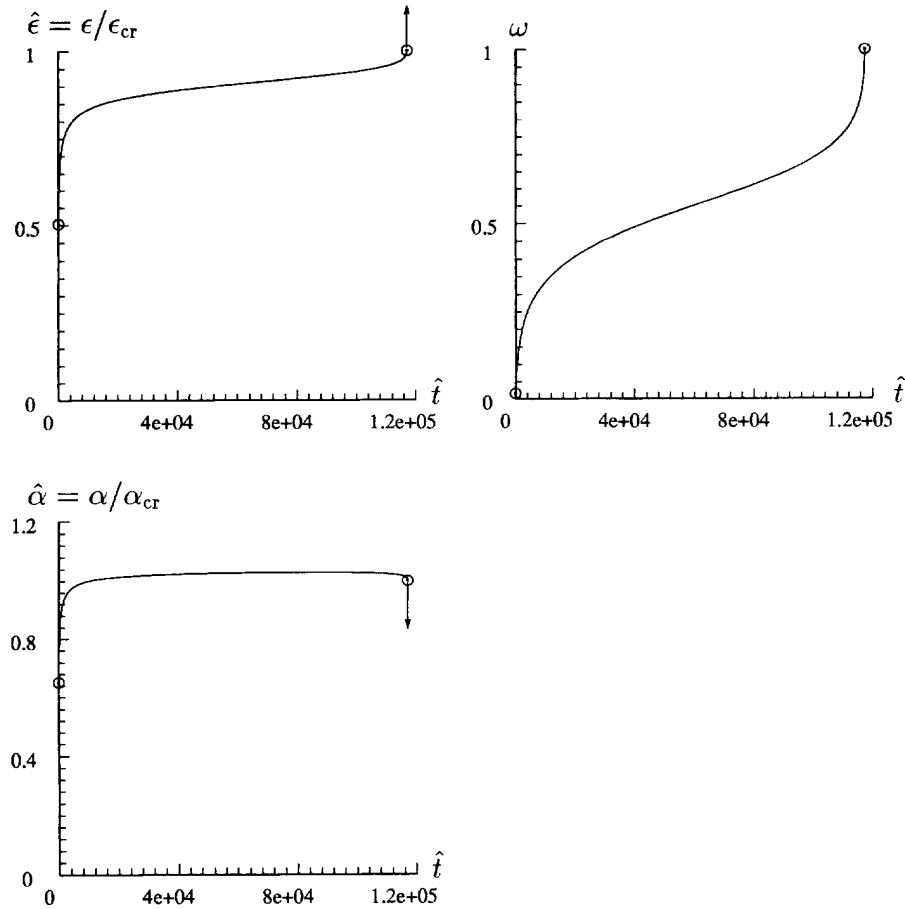
The response of the system as $\omega \to 1$ is such that

Fig. 1. Temporal variations of the strain ε, the damage parameter ω, and the back stress α for uniaxial tension test with values of $E_f/E_m = 3, f = 35\%, n = 3, m = 5$, and $\sigma/S_c = 0.25$.

$$\varepsilon \to \varepsilon_{cr}, \quad \dot{\varepsilon} \to \infty, \quad \alpha \to \alpha_{cr}, \quad \text{and} \quad \dot{\alpha} \to -\infty, \tag{11}$$

where

$$\varepsilon_{cr} = \frac{S_c}{E_f}\left(\frac{2}{m+2}\frac{E}{fE_f}\right)^{1/(m+1)} \quad \text{and} \quad \alpha_{cr} = fE_f\left(1 - \frac{1}{m+2}\frac{E}{fE_f}\right)\varepsilon_{cr}. \tag{12}$$

Equation (11d) shows that, at $\omega = 1$ the fibers are suddenly unloaded and the load is transferred instantaneously to the matrix.

We consider next the case of a 'creep test' in which a constant tensile stress σ is applied in the direction of the fibers. Equations (7) are integrated numerically and the evolution of the solution is determined until ω reaches the value of one. Figure 1 shows the temporal variation of ε, α, and ω for $E_f/E_m = 3$, $f = 0.35$, $n = 3$, $m = 5$, and $\sigma/S_c = 0.25$; the normalized quantities used in Fig. 1 are defined as

$$\hat{\varepsilon} = \varepsilon/\varepsilon_{cr}, \quad \hat{\alpha} = \alpha/\alpha_{cr}, \quad \text{and} \quad \hat{t} = tB'E_fS_c^{n-1}. \tag{13}$$

We conclude this section with a discussion of the case where the applied uniaxial stress σ is such that the corresponding axial strain does not increase monotonically with time. In such a case, the fraction of broken fibers on any cross-section depends on both the current value of the applied stress σ and the maximum value of σ in the loading history of the specimen. Equation (2a) is now replaced by (Cheng, 1996)

$$\bar{\sigma}_f(\varepsilon) = \left\{ 1 - \frac{\beta \sigma_f^{un}(\varepsilon)}{S_c} \left[\frac{\sigma_{fmax}^{un}(\varepsilon)}{S_c} \right]^m \right\} \sigma_f^{un}(\varepsilon),$$ (14)

where $\sigma_f^{un}(\varepsilon) = E_f \varepsilon$, $\sigma_{fmax}^{un}(\varepsilon)$ is the maximum tensile value of σ_f^{un} in the loading history of the specimen $(\sigma_{fmax}^{un} \geqslant 0)$, and

$$\beta = \begin{cases} 1 & \text{if } \varepsilon > 0, \\ 0 & \text{if } \varepsilon \leqslant 0. \end{cases}$$ (15)

The conditions given in eqn (15) above are based on the assumption that fiber breaks affect the material response in tension but have no effect when the specimen is loaded in compression along the fibers. The corresponding definitions of ω and E_f^{tan} are

$$\omega(\varepsilon) = (m+2) \frac{f E_f}{E} \frac{\beta \sigma_f^{un}(\varepsilon)}{2 S_c} \left[\frac{\sigma_{fmax}^{un}(\varepsilon)}{S_c} \right]^m,$$ (16)

and

$$E_f^{tan} = \frac{d\bar{\sigma}_f}{d\varepsilon} = \left(1 - \frac{\lambda m + 2}{m+2} \frac{E}{f E_f} \omega \right) E_f.$$ (17)

Using the definition of ω, we can readily show that

$$\dot{\omega} = (\lambda m + 1) \omega \frac{\dot{\sigma}_f^{un}}{\sigma_f^{un}} \quad \text{where } \lambda = \begin{cases} 1 & \text{if } \sigma_f^{un} = \sigma_{fmax}^{un} \quad \text{and} \quad \dot{\varepsilon} > 0, \\ 0 & \text{otherwise.} \end{cases}$$ (18)

In deriving eqn (18a), we took into account that $\lambda \sigma_{fmax}^{un} = \lambda \sigma_f^{un}$. Finally, using the above results, we can show that the evolution equations for the axial strain and the back stress become

$$\dot{\varepsilon} = \frac{\dot{\alpha}}{f E_f^{tan}} = \frac{\dot{\sigma}}{E_L} + \frac{B E_m}{(1-f)^{n-1} E_L} |\sigma - \alpha|^{n-1} (\sigma - \alpha),$$ (19)

where

$$E_L = f E_f^{tan} + (1-f) E_m = \left(1 - \frac{\lambda m + 2}{m+2} \omega \right) E.$$ (20)

Note that, when $\varepsilon > 0$, $\sigma_f^{un} \equiv E_f \varepsilon = \sigma_{fmax}^{un}$ and $\dot{\varepsilon} > 0$, then $\beta = \lambda = 1$, $E_L = (1-\omega)E$ and eqns (19) reduce to (7). Also, as the damage parameter ω approaches unity $(\omega \to 1)$, $\lambda = 1$ and $E_L = (1-\omega)E \to 0$, so that $\dot{\varepsilon} \to \infty$.

2.2. A three-dimensional version of the McLean model with damage

Here, we proceed in a way similar to that used in Section 4.2. of Part I, where there was no damage. The applied macroscopic load is axisymmetric of the form shown in Fig. 1b of Part I, i.e. $\sigma_{1'1'} = \sigma_{2'2'} = \sigma_p$ and $\sigma_{33} = \sigma_n$. We assume again that the stresses in the fibers and the matrix are *uniform* and of the form

$$[\boldsymbol{\sigma}_f] = \begin{bmatrix} \sigma_p & 0 & 0 \\ 0 & \sigma_p & 0 \\ 0 & 0 & \bar{\sigma}_f \end{bmatrix} \quad \text{and} \quad [\boldsymbol{\sigma}_m] = \begin{bmatrix} \sigma_p & 0 & 0 \\ 0 & \sigma_p & 0 \\ 0 & 0 & \sigma_m \end{bmatrix}. \tag{21}$$

Using equation (5a) of Part I, we readily conclude that

$$\sigma_n = f\bar{\sigma}_f + (1-f)\sigma_m \quad \text{or} \quad \sigma_m = \frac{\sigma_n - \alpha}{1-f}, \tag{22}$$

where the back stress is defined again as $\alpha = f\bar{\sigma}_f$. It is also assumed that the corresponding axial strain component in the fibers and the matrix is equal to the axial macroscopic strain $\varepsilon_{33} = \varepsilon_n$, i.e.,

$$\varepsilon_{f33} = \varepsilon_{m33} = \varepsilon_n. \tag{23}$$

Equation (5b) of Part I implies that

$$\begin{Bmatrix} \dot{\varepsilon}_{11} \\ \dot{\varepsilon}_{22} \\ \dot{\varepsilon}_{33} \end{Bmatrix} = f \begin{Bmatrix} \dot{\varepsilon}^f_{11} \\ \dot{\varepsilon}^f_{22} \\ \dot{\varepsilon}^f_{33} \end{Bmatrix} + (1-f) \begin{Bmatrix} \dot{\varepsilon}^m_{11} \\ \dot{\varepsilon}^m_{22} \\ \dot{\varepsilon}^m_{33} \end{Bmatrix}. \tag{24}$$

The damage parameter ω is defined again as

$$\omega(\varepsilon_n, \sigma_p) = (m+2) \frac{fE_f}{E} \frac{\beta\sigma_f^{un}(\varepsilon_n, \sigma_p)}{2S_c} \left[\frac{\sigma_{fmax}^{un}(\varepsilon_n, \sigma_p)}{S_c} \right]^m, \tag{25}$$

so that

$$\dot{\omega} = (\lambda m + 1)\omega \frac{\dot{\sigma}_f^{un}}{\sigma_f^{un}}, \tag{26}$$

where now

$$\sigma_f^{un}(\varepsilon_n, \sigma_p) = E_f \varepsilon_n + 2v_f \sigma_p, \tag{27}$$

and β and λ take the values of 1 or 0 according to eqns (15) with $\varepsilon = \varepsilon_n$, and (18b) with σ_f^{un} defined by eqn (27) above.

The average stress in the fibers is given by eqn (14), which can be written as

$$\bar{\sigma}_f = (1 - c\omega)\sigma_f^{un} \quad \text{where} \quad c = \frac{1}{m+2} \frac{E}{fE_f}. \tag{28}$$

Using an argument similar to that used by Hild et al. (1992), we readily conclude that the elastic constitutive equation for the damaged fibers can be written as

$$\begin{Bmatrix} \varepsilon^f_{11} \\ \varepsilon^f_{22} \\ \varepsilon^f_{33} \end{Bmatrix} = \frac{1}{E_f} \begin{bmatrix} 1 & -v_f & -v_f \\ -v_f & 1 & -v_f \\ -v_f & -v_f & 1/(1-c\omega) \end{bmatrix} \begin{Bmatrix} \sigma_p \\ \sigma_p \\ \bar{\sigma}_f \end{Bmatrix}. \tag{29}$$

Since the damage parameter ω is a non-linear function of ε_n and σ_p (see eqns (25) and (27) above), the last equation can be viewed as a non-linear transversely isotropic elastic

constitutive equation that relates the average stress to the average strain in the fibers. Equation (24) now becomes

$$
\begin{Bmatrix} \dot{\varepsilon}_{11} \\ \dot{\varepsilon}_{22} \\ \dot{\varepsilon}_{33} \end{Bmatrix} = \frac{f}{E_f} \begin{bmatrix} 1 & -v_f & -v_f \\ -v_f & 1 & -v_f \\ -v_f & -v_f & 1/(1-c\omega) \end{bmatrix} \begin{Bmatrix} \dot{\sigma}_p \\ \dot{\sigma}_p \\ \dot{\sigma}_f \end{Bmatrix} + \frac{f}{E_f} \begin{bmatrix} 0 & 0 & 0 \\ 0 & 0 & 0 \\ 0 & 0 & c\dot{\omega}/(1-c\omega) \end{bmatrix} \begin{Bmatrix} \sigma_p \\ \sigma_p \\ \sigma_f \end{Bmatrix}
$$

$$
+ \frac{1-f}{E_m} \begin{bmatrix} 1 & -v_m & -v_m \\ -v_m & 1 & -v_m \\ -v_m & -v_m & 1 \end{bmatrix} \begin{Bmatrix} \dot{\sigma}_p \\ \dot{\sigma}_p \\ \dot{\sigma}_m \end{Bmatrix} + (1-f)\frac{B}{2} |\sigma_m - \sigma_p|^{n-1} (\sigma_m - \sigma_p) \begin{Bmatrix} -1 \\ -1 \\ 2 \end{Bmatrix}. \tag{30}
$$

Using a procedure similar to that of Part I, we substitute first the constitutive equations for the fibers and the matrix in the strain continuity equation $\dot{\varepsilon}_{f33} = \dot{\varepsilon}_{m33}$. Equations (22b), (26) and (27) are then used to eliminate σ_m and $\dot{\omega}$, and the resulting equation is used to determine $\dot{\alpha}$ in terms of $\dot{\sigma}_n$, $\dot{\sigma}_p$, σ_n, σ_p and α. Finally, substituting the expression for $\dot{\alpha}$ into (30) and using (22b), (26) and (27) to eliminate σ_m and $\dot{\omega}$, we obtained the following equation for the macroscopic strain rates:

$$
\begin{Bmatrix} \dot{\varepsilon}_{11} \\ \dot{\varepsilon}_{22} \\ \dot{\varepsilon}_{33} \end{Bmatrix} = \begin{bmatrix} 1/E_T & -v_T/E_T & -v_L/E_L \\ -v_T/E_T & 1/E_T & -v_L/E_L \\ -v_L/E_L & -v_L/E_L & 1/E_L \end{bmatrix} \begin{Bmatrix} \dot{\sigma}_p \\ \dot{\sigma}_p \\ \dot{\sigma}_n \end{Bmatrix} + \frac{3}{2} B(1-f) \left| \frac{\sigma_n - \alpha}{1-f} - \sigma_p \right|^{n-1} \left(\frac{\sigma_n - \alpha}{1-f} - \sigma_p \right) \begin{Bmatrix} K \\ K \\ L \end{Bmatrix},
$$

$$
\tag{31}
$$

where

$$
E_L = f E_f^{tan} + (1-f)E_m, \qquad v_L = f\tilde{v}_f + (1-f)v_m, \tag{32}
$$

$$
\frac{1}{E_T} = \frac{1-f}{E_m} + \frac{f}{E_f} + 2f(1-f)\frac{E_f^{tan}}{E_L}\left(\frac{E_m}{E_f}v_f - v_m\right)\left(\frac{v_m}{E_m} - \frac{v_f}{E_f}\right), \tag{33}
$$

$$
\frac{v_T}{E_T} = (1-f)\frac{v_m}{E_m} + f\frac{v_f}{E_f}, \tag{34}
$$

$$
E_f^{tan} = \left(1 - \frac{\lambda m + 2}{m+2}\frac{E}{f E_f}\omega\right)E_f, \qquad \tilde{v}_f = \left(1 - \frac{\lambda m + 2}{m+2}\frac{E}{f E_f}\omega\right)v_f, \tag{35}
$$

and

$$
K = \frac{2}{3}\frac{E_m}{E_L}\left\{-\frac{1}{2} + f\left[\frac{E_f^{tan}}{E_m}\left(v_m - \frac{1}{2}\right) - \left(\tilde{v}_f - \frac{1}{2}\right)\right]\right\}, \qquad L = \frac{2}{3}\frac{E_m}{E_L}. \tag{36}
$$

The evolution equation of the back stress ($\dot{\alpha} = f\dot{\sigma}_f$) is found to be

$$
\frac{\dot{\alpha}}{f E_f^{tan}} = \frac{\dot{\sigma}_n}{E_L} + 2(1-f)\left(\frac{E_m}{E_f}v_f - v_m\right)\frac{\dot{\sigma}_p}{E_L} + \frac{B E_m(1-f)}{E_L}\left|\frac{\sigma_n - \alpha}{1-f} - \sigma_p\right|^{n-1}\left(\frac{\sigma_n - \alpha}{1-f} - \sigma_p\right). \tag{37}
$$

3. A PROPOSED NEW MODEL

The results developed in the previous section are now incorporated in a three-dimensional constitutive model. As mentioned in the introduction, we assume that fiber failure does not affect significantly the response of the composite when shear loads relative to the

fibers are applied, so that equations (16)–(19) of Part I can still be used for such types of loading.

The macroscopic response of the composite is assumed to be transversely isotropic, and the unit vector $\mathbf{n}$ in the direction of the fibers is used to define the axis of rotational symmetry. The total strain in the composite is written as the sum of the elastic and creep parts:

$$\boldsymbol{\varepsilon} = \boldsymbol{\varepsilon}^e + \boldsymbol{\varepsilon}^{cr}. \tag{38}$$

In the following, we discuss the constitutive equations for $\dot{\boldsymbol{\varepsilon}}^e$ and $\dot{\boldsymbol{\varepsilon}}^{cr}$ for the composite.

3.1. *Elasticity*

The elastic constitutive equation can be written in rate form as

$$\dot{\boldsymbol{\varepsilon}}^e = \mathbf{C}^{e-1} : \dot{\boldsymbol{\sigma}}, \tag{39}$$

where the fourth-order tangent elasticity tensor $\mathbf{C}^e(\omega, \lambda)$ for the homogenized transversely isotropic composite depends, in general, on the current value of the damage parameter ω and the direction of loading through λ.

When the fibers are aligned with the x_3 coordinate direction (i.e., $\mathbf{n} = \mathbf{e}_3$), eqn (39) can be written in matrix form as follows

$$\{\boldsymbol{\varepsilon}^e\} = [C^e]^{-1}\{\boldsymbol{\sigma}\}, \tag{40}$$

where $\{\dot{\varepsilon}^e\} = \{\dot{\varepsilon}^e_{11}, \dot{\varepsilon}^e_{22}, \dot{\varepsilon}^e_{33}, \dot{\gamma}^e_{12}, \dot{\gamma}^e_{13}, \dot{\gamma}^e_{23}\}$, $\{\dot{\sigma}\} = \{\dot{\sigma}_{11}, \dot{\sigma}_{22}, \dot{\sigma}_{33}, \dot{\sigma}_{12}, \dot{\sigma}_{13}, \dot{\sigma}_{23}\}$, and

$$[C^e]^{-1} = \begin{bmatrix} 1/E_T & -v_T/E_T & -v_L/E_L & 0 & 0 & 0 \\ -v_T/E_T & 1/E_T & -v_L/E_L & 0 & 0 & 0 \\ -v_L/E_L & -v_L/E_L & 1/E_L & 0 & 0 & 0 \\ 0 & 0 & 0 & 1/G_T & 0 & 0 \\ 0 & 0 & 0 & 0 & 1/G_L & 0 \\ 0 & 0 & 0 & 0 & 0 & 1/G_L \end{bmatrix},$$

where E_L, E_T, G_L, v_L and v_T are the five independent elastic moduli of the composite, and

$$G_T = \frac{E_T}{2(1+v_T)}. \tag{41}$$

The moduli E_L, E_T, v_L and v_T are defined in eqns (32)–(35); the shear modulus G_L is assumed to be independent of ω and is estimated by (Christensen, 1979, p. 84)

$$G_L = \frac{(1+f)G_f + (1-f)G_m}{(1-f)G_f + (1+f)G_m} G_m, \tag{42}$$

where G_m and G_f are the elastic shear moduli of the matrix and the fibers.

The constitutive equations developed here have a form similar to that of Part I. It should be emphasized though, that the effective elastic tangent moduli are now strong functions of the damage parameter ω. When $\omega = 0$, the above equations reduce to those presented in Part I; also, in the limit as $\omega \to 1$, the effective tangent modulus E_L approaches zero, and $\dot{\boldsymbol{\varepsilon}}^e$ becomes infinite.

3.2. Creep

The general form of the constitutive equations that account for fiber failure during creep is

$$\dot{\varepsilon}^{cr} = \mathbf{g}(\boldsymbol{\sigma} - \boldsymbol{\alpha}, \boldsymbol{\omega}, \lambda, s), \tag{43}$$

where $\boldsymbol{\alpha}$ is the back stress tensor, $\boldsymbol{\omega}$ is the damage tensor, $\mathbf{g}$ is a tensor-valued isotropic functions, s is the collection of material parameters $s = \{E_f, v_f, E_m, v_m, B, n, f, S_c, m\}$.

In the present model, the back stress $\boldsymbol{\alpha}$ and the damage tensor $\boldsymbol{\omega}$ are assumed to be in the direction of $\mathbf{n}$, i.e., $\boldsymbol{\alpha} = \alpha\mathbf{nn}$, $\boldsymbol{\omega} = \omega\mathbf{nn}$; it should be noted, however, that more complicated forms may be necessary when effects such as fiber debonding must be accounted for.

In the following, we use the results of Section 3.3 of Part I for shear loads together with those of Section 2.2 in the present paper for axisymmetric loading and develop constitutive equations for general types of loading. These results are combined in a way similar to that used in Part I. With respect to the coordinate axes shown in Fig. 1 of Part I and for an arbitrary orientation of the x_1-x_2 axes on the transverse plane, we write the following equations for the creep strain rate:

$$[\dot{\varepsilon}^{cr}] = \frac{3}{2} B(1-f) \Sigma_c^{n-1} \begin{bmatrix} \chi(\sigma_{11} - \sigma_{22})/2 + KS & \chi\sigma_{12} & \chi\sigma_{13} \\ \chi\sigma_{12} & \chi(\sigma_{22} - \sigma_{11})/2 + KS & \chi\sigma_{23} \\ \chi\sigma_{13} & \chi\sigma_{23} & LS \end{bmatrix}, \tag{44}$$

where $\Sigma_c^2 = S^2 + (\chi\sigma_s)^2$. For convenience, we repeat the definition of the quantities entering the above equation: $\sigma_n = \sigma_{33}$, $\sigma_p = (\sigma_{11} + \sigma_{22})/2$,

$$S = \frac{\sigma_n - \alpha}{1-f} - \sigma_p, \qquad \sigma_s^2 = \frac{3}{4}(\sigma_{11} - \sigma_{22})^2 + 3(\sigma_{12}^2 + \sigma_{13}^2 + \sigma_{23}^2). \tag{45}$$

The quantity $\chi(n, f)$ is given by equations (17)–(19) of Part I, and K and L are defined in eqn (36) in the present paper.

The constitutive equations developed here have a form similar to that of Part I. It should be emphasized though, that K and L are now strong functions of the damage parameter ω. When $\omega = 0$, the above equations reduce to those presented in Part I; whereas, in the limit as $\omega \rightarrow 1$, the effective tangent modulus E_L approaches zero, and, as a consequence, K, L and $\dot{\varepsilon}^{cr}$ become infinite.

3.3. The evolution of the back stress and the damage parameter

The general form of the constitutive equations for $\dot{\boldsymbol{\alpha}}$ and $\boldsymbol{\omega}$ are

$$\dot{\boldsymbol{\alpha}} = \mathbf{h}(\boldsymbol{\sigma} - \boldsymbol{\alpha}, \dot{\boldsymbol{\sigma}}, \boldsymbol{\omega}, \lambda, s), \qquad \boldsymbol{\omega} = \mathbf{r}(\boldsymbol{\sigma}, \boldsymbol{\varepsilon}, \text{history}, s), \tag{46}$$

where $\mathbf{h}$ and $\mathbf{r}$ are tensor-valued isotropic functions, and the argument 'history' in $\mathbf{r}$ denotes dependence on the history of deformation.

As mentioned earlier, the back stress $\boldsymbol{\alpha}$ and the damage tensor $\boldsymbol{\omega}$ are assumed to be of the form $\boldsymbol{\alpha} = \alpha\mathbf{nn}$, and $\boldsymbol{\omega} = \omega\mathbf{nn}$.

The evolution of α is given by

$$\frac{\dot{\alpha}}{fE_f^{tan}} = \frac{\dot{\sigma}_n}{E_L} + 2(1-f)\left(\frac{E_m}{E_f}v_f - v_m\right)\frac{\dot{\sigma}_p}{E_L} + \frac{BE_m(1-f)}{E_L} \Sigma_c^{n-1}\left(\frac{\sigma_n - \alpha}{1-f} - \sigma_p\right), \tag{47}$$

where $\Sigma_c^2 = S^2 + (\chi\sigma_s)^2$.

The damage parameter ω is defined as

$$\omega(\varepsilon_n, \sigma_p) = (m+2)\frac{fE_f}{E}\frac{\beta\sigma_f^{un}(\varepsilon_n, \sigma_p)}{2S_c}\left[\frac{\sigma_{fmax}^{un}(\varepsilon_n, \sigma_p)}{S_c}\right]^m, \tag{48}$$

where

$$\sigma_f^{un}(\varepsilon_n, \sigma_p) = E_f\varepsilon_n + 2v_f\sigma_p, \quad \text{and} \quad \beta = \begin{cases} 1 & \text{if } \varepsilon_n > 0, \\ 0 & \text{if } \varepsilon_n \leqslant 0. \end{cases} \tag{49}$$

The parameter λ that enters the expressions of E_f^{tan} and $\tilde{v}_f$ is defined as

$$\lambda = \begin{cases} 1 & \text{if } \sigma_f^{un} = \sigma_{fmax}^{un} \quad \text{and} \quad \dot{\varepsilon}_n > 0, \\ 0 & \text{otherwise.} \end{cases} \tag{50}$$

The instantaneous response of the composite to applied loads is 'purely elastic'. The values of the strain $\varepsilon_0 = \varepsilon_0^e$, the back stress α_0, and the damage parameter ω_0 immediately after the application of the load are determined from the integration of eqns (39), (47), and the use of eqn (48) respectively; these values are the three dimensional counterparts of the quantities in eqn (9) for the case of uniaxial tension.

4. FINITE ELEMENT IMPLEMENTATION OF THE CONSTITUTIVE MODEL

In this section, we discuss the implementation of the general form of the constitutive model described in the previous section in a finite element program. In a finite element environment, the solution of the creep problem is developed incrementally and the constitutive equations are integrated at the element Gauss points. In a displacement based finite element formulation the solution is deformation driven. At a material point, the solution $(\sigma_n, \varepsilon_n, \alpha_n, \omega_n)$ at time t_n as well as the strain ε_{n+1} at time $t_{n+1} = t_n + \Delta t$ are supposed to be known and one has to determine the solution $(\sigma_{n+1}, \alpha_{n+1}, \omega_{n+1})$.

4.1. Numerical integration of the constitutive equations

We used the backward Euler method to integrate the evolution equations for ε^e, ε^{cr}, and α. Starting with the elasticity eqn (39) we write

$$\sigma_{n-1} = \sigma_n + C^e(\omega_{n+1}, \lambda) : \Delta\varepsilon^e = \sigma_n + C^e(\omega_{n+1}, \lambda) : (\Delta\varepsilon - \Delta\varepsilon^{cr}), \tag{51}$$

where $\Delta\varepsilon = \varepsilon_{n+1} - \varepsilon_n$ and $\Delta\varepsilon^{cr} = \varepsilon_{n-1}^{cr} - \varepsilon_n^{cr}$ are the total- and creep-strain increments. The other constitutive equations are written as

$$\Delta\varepsilon^{cr} = g(\sigma_{n+1} - \alpha_{n+1}, \omega_{n+1}, \lambda)\,\Delta t, \tag{52}$$

$$\Delta\alpha = h(\sigma_{n-1} - \alpha_{n+1}, \Delta\sigma/\Delta t, \omega_{n+1}, \lambda)\,\Delta t, \tag{53}$$

$$\omega_{n+1} = r(\sigma_{n-1}, \varepsilon_{n+1}), \tag{54}$$

where $\Delta\sigma = \sigma_{n+1} - \sigma_n$. The value of λ for the increment is determined as described in the following. Let σ_{fmax}^{un} be the maximum local non-negative value of σ_f^{un} in the history of deformation up to time t_n at the start of the increment. Then

$$\lambda = \begin{cases} 1 & \text{if } (\sigma_f^{un})_{n+1} > \sigma_{fmax}^{un}, \quad \text{and} \quad \varepsilon_{n+1} > \varepsilon_n, \\ 0 & \text{otherwise} \end{cases} \tag{55}$$

where

$$(\sigma_f^{un})_{n+1} = E_f(\varepsilon_n)_{n+1} + 2v_f(\sigma_p)_{n+1}, \tag{56}$$

$(\varepsilon_n)_{n+1} = \mathbf{n} \cdot \boldsymbol{\varepsilon}_{n+1} \cdot \mathbf{n}$, $(\sigma_p)_{n+1} = (1/2)\sigma_{n+1}$: $(\mathbf{I} - \mathbf{nn})$, $\mathbf{n}$ is the unit vector in the direction of the fibers, and $\mathbf{I}$ is the second-order identity tensor. Also, the function $r(\sigma_{n+1}, \boldsymbol{\varepsilon}_{n+1})$ is defined as

$$r(\sigma_{n+1}, \boldsymbol{\varepsilon}_{n+1}) = (m+2)\frac{fE_f}{2E}\frac{\beta(\sigma_f^{un})_{n+1}}{S_c}\left(\frac{\sigma_{fmax}^{un}}{S_c}\right)^m \tag{57}$$

where

$$\beta = \begin{cases} 1 & \text{if } (\varepsilon_n)_{n+1} > 0, \\ 0 & \text{if } (\varepsilon_n)_{n+1} \leqslant 0. \end{cases} \tag{58}$$

At the start of an increment the value of $(\sigma_p)_n$ is used in (56) instead of $(\sigma_p)_{n+1}$, and λ is set to either unity or zero according to (55). At the end of the integration the determined value of $(\sigma_p)_{n+1}$ is used in (56) in order to check the correctness of the used value for λ.

Summarizing, we write

$$\mathbf{G}(\Delta\boldsymbol{\varepsilon}^{cr}, \Delta\boldsymbol{\alpha}, \omega_{n+1}) \equiv \Delta\boldsymbol{\varepsilon}^{cr} - \Delta t\mathbf{g}(\sigma_{n+1} - \boldsymbol{\alpha}_n - \Delta\boldsymbol{\alpha}, \omega_{n+1}, \lambda) = 0, \tag{59}$$

$$\mathbf{H}(\Delta\boldsymbol{\varepsilon}^{cr}, \Delta\boldsymbol{\alpha}, \omega_{n+1}) \equiv \Delta\boldsymbol{\alpha} - \Delta t\mathbf{h}\left(\sigma_{n+1} - \boldsymbol{\alpha}_n - \Delta\boldsymbol{\alpha}, \frac{\sigma_{n+1} - \sigma_n}{\Delta t}, \omega_{n+1}, \lambda\right) = 0, \tag{60}$$

$$R(\Delta\boldsymbol{\varepsilon}^{cr}, \Delta\boldsymbol{\alpha}, \omega_{n+1}) \equiv \omega_{n+1} - r(\sigma_{n+1}, \boldsymbol{\varepsilon}_{n+1}) = 0, \tag{61}$$

where

$$\sigma_{n+1}(\Delta\boldsymbol{\varepsilon}^{cr}, \omega_{n+1}) = \sigma_n + \mathbf{C}^e(\omega_{n+1}, \lambda) : (\Delta\boldsymbol{\varepsilon} - \Delta\boldsymbol{\varepsilon}^{cr}). \tag{62}$$

We choose $\Delta\boldsymbol{\varepsilon}^{cr}$, $\Delta\boldsymbol{\alpha}$, and ω_{n+1} as the primary unknowns and treat (59)–(61) as the basic equations in which σ_{n+1} is defined by (62). The solution is obtained by using Newton's method. The first estimates for $\Delta\boldsymbol{\varepsilon}^{cr}$ and $\Delta\boldsymbol{\alpha}$ used to start the Newton loop are obtained by using a forward Euler scheme, i.e., $(\Delta\boldsymbol{\varepsilon}^{cr})_{est} = \mathbf{g}(\sigma_n - \boldsymbol{\alpha}_n, \omega_n, \lambda_n)\Delta t$ and $(\Delta\boldsymbol{\alpha})_{est} = \mathbf{h}(\sigma_n - \boldsymbol{\alpha}_n, \Delta\sigma_n/\Delta t, \omega_n, \lambda_n)\Delta t$, where $\Delta\sigma_n = \sigma_n - \sigma_{n-1}$; also the first estimate for ω_{n+1} is given by $(\omega)_{est} = r(\sigma_n, \boldsymbol{\varepsilon}_{n+1})$.

Once $\Delta\boldsymbol{\varepsilon}^{cr}$, $\Delta\boldsymbol{\alpha}$, and ω_{n+1} are found, eqn (62) defines the stress σ_{n+1}, $\boldsymbol{\alpha}_{n+1} = \boldsymbol{\alpha}_n + \Delta\boldsymbol{\alpha}$, and this completes the integration procedure.

The case of plane stress is related in a way similar to that described in Section 6.3 of Part I.

We conclude this section with a discussion of the numerical treatment of the limiting case $\omega = 1$. As ω approaches unity, the strain rate approaches infinity, thus introducing numerical difficulties. In our finite element calculations, the damage parameter ω was not permitted to grow beyond a critical value, say $\omega_{cr} = 0.99$. Once this critical value was reached at an integration point, ω was kept equal to ω_{cr} and the corresponding back stress α was let to evolve until the value $\alpha = 0$, corresponding to complete fiber unloading, was reached; the calculations were continued beyond this point with $\omega = \omega_{cr}$ and $\alpha = 0$.

4.2. Linearization moduli

In an implicit finite element code, the overall discretized equilibrium equations are written at the end of the increment, resulting in a set of nonlinear equations for the nodal unknowns. If a full Newton scheme is used to solve the global nonlinear equations, one needs to calculate the so-called 'linearization moduli' $\mathscr{J}$

$$\mathscr{J} = \frac{\partial \boldsymbol{\sigma}_{n+1}}{\partial \boldsymbol{\varepsilon}_{n+1}}. \tag{63}$$

For simplicity, we drop the subscript $(n+1)$ with the understanding that all quantities are evaluated at the end of the increment, unless otherwise indicated. Starting with the elasticity eqn (51), we find

$$\partial \boldsymbol{\sigma} = \frac{\partial \mathbf{C}^e}{\partial \omega} : \Delta \boldsymbol{\varepsilon}^e \, \partial \omega + \mathbf{C}^e : (\partial \boldsymbol{\varepsilon} - \partial \boldsymbol{\varepsilon}^{cr}), \tag{64}$$

where $\Delta \boldsymbol{\varepsilon}^e = \boldsymbol{\varepsilon}^e_{n+1} - \boldsymbol{\varepsilon}^e_n$ The differentials $\partial \boldsymbol{\varepsilon}^{cr}$, $\partial \boldsymbol{\alpha}$ and $\partial \omega$ are evaluated from eqns (52)–(54) as follows:

$$\partial \boldsymbol{\varepsilon}^{cr} = \Delta t \left[\frac{\partial \mathbf{g}}{\partial \mathbf{s}} : (\partial \boldsymbol{\sigma} - \partial \boldsymbol{\alpha}) + \frac{\partial \mathbf{g}}{\partial \omega} \, \partial \omega \right], \tag{65}$$

$$\partial \boldsymbol{\alpha} = \Delta t \left[\frac{\partial \mathbf{h}}{\partial \mathbf{s}} : (\partial \boldsymbol{\sigma} - \partial \boldsymbol{\alpha}) + \frac{1}{\Delta t} \frac{\partial \mathbf{h}}{\partial \dot{\boldsymbol{\sigma}}} : \partial \boldsymbol{\sigma} + \frac{\partial \mathbf{h}}{\partial \omega} \, \partial \omega \right], \tag{66}$$

$$\partial \omega = \frac{\partial r}{\partial \boldsymbol{\sigma}} : \partial \boldsymbol{\sigma} + \frac{\partial r}{\partial \boldsymbol{\varepsilon}} : \partial \boldsymbol{\varepsilon}, \tag{67}$$

where $\mathbf{s} = \boldsymbol{\sigma} - \boldsymbol{\alpha}$. Using (67) to define $\partial \omega$, we can solve (65) and (66) for $\partial \boldsymbol{\alpha}$ and $\partial \boldsymbol{\varepsilon}^{cr}$ to find

$$\partial \boldsymbol{\alpha} = \mathbf{A} : \partial \boldsymbol{\sigma} + \mathbf{B} : \partial \boldsymbol{\varepsilon}, \tag{68}$$

$$\partial \boldsymbol{\varepsilon}^{cr} = \mathbf{D} : \partial \boldsymbol{\sigma} + \mathbf{E} : \partial \boldsymbol{\varepsilon}, \tag{69}$$

where

$$\mathbf{A} = \Delta t \left(\mathbf{J} + \Delta t \frac{\partial \mathbf{h}}{\partial \mathbf{s}} \right)^{-1} : \left(\frac{\partial \mathbf{h}}{\partial \mathbf{s}} + \frac{1}{\Delta t} \frac{\partial \mathbf{h}}{\partial \dot{\boldsymbol{\sigma}}} + \frac{\partial \mathbf{h}}{\partial \omega} \frac{\partial r}{\partial \boldsymbol{\sigma}} \right), \tag{70}$$

$$\mathbf{B} = \Delta t \left(\mathbf{J} + \Delta t \frac{\partial \mathbf{h}}{\partial \mathbf{s}} \right)^{-1} : \frac{\partial \mathbf{h}}{\partial \omega} \frac{\partial r}{\partial \boldsymbol{\varepsilon}}, \tag{71}$$

$$\mathbf{D} = \Delta t \left[\frac{\partial \mathbf{g}}{\partial \mathbf{s}} : (\mathbf{J} - \mathbf{A}) + \frac{\partial \mathbf{g}}{\partial \omega} \frac{\partial r}{\partial \boldsymbol{\sigma}} \right], \quad \mathbf{E} = \Delta t \left(-\frac{\partial \mathbf{g}}{\partial \mathbf{s}} : \mathbf{B} + \frac{\partial \mathbf{g}}{\partial \omega} \frac{\partial r}{\partial \boldsymbol{\varepsilon}} \right), \tag{72}$$

$\mathbf{J}$ being the fourth-order identity tensor.

Finally, substituting the expression for $\partial \boldsymbol{\varepsilon}^{cr}$ into (64) and solving for $\partial \boldsymbol{\sigma} / \partial \boldsymbol{\varepsilon}$, we find

$$\mathscr{J} = \left(\mathbf{J} + \mathbf{C}^e : \mathbf{D} - \frac{\partial \mathbf{C}^e}{\partial \omega} : \Delta \boldsymbol{\varepsilon}^e \frac{\partial r}{\partial \boldsymbol{\sigma}} \right)^{-1} : \left(\mathbf{C}^e - \mathbf{C}^e : \mathbf{E} + \frac{\partial \mathbf{C}^e}{\partial \omega} : \Delta \boldsymbol{\varepsilon}^e \frac{\partial r}{\partial \boldsymbol{\varepsilon}} \right). \tag{73}$$

5. AN EXAMPLE: A PLATE WITH A HOLE

The model developed in Section 3 is implemented in the ABAQUS general-purpose finite element program (Hibbitt, 1984). The constitutive equations are integrated by using the method presented in Section 4.

The problem of a plate with a hole discussed in Section 7 of Part I is analyzed again, using the new constitutive model that accounts for fiber failure. The same geometry,
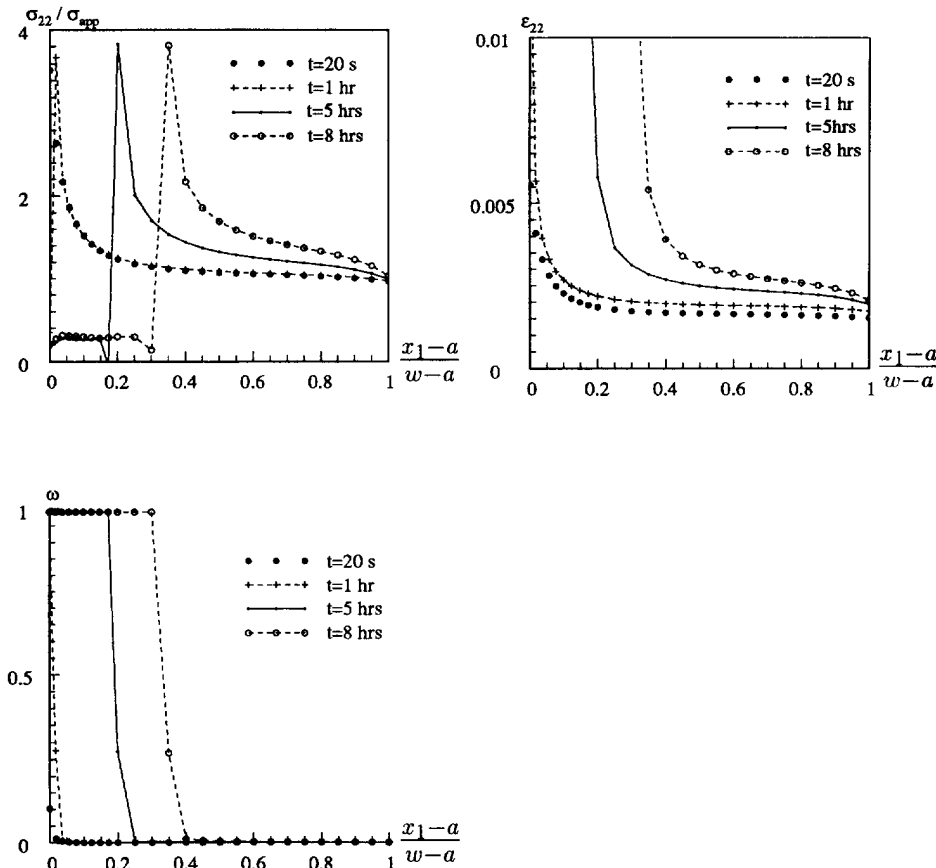
Fig. 2. Variations of the axial stress σ_{22}/σ_{app}, the axial strain ε_{22}, and the damage parameter ω along
the cross-fiber direction at time $t = 20$ sec, 1, 5 and 8 hours.

material properties, and finite element mesh are used. The fiber diameter is assumed to be
$D = 100\ \mu\text{m}$. The Weibull modulus of the fibers is $m = 5$, and the gauge strength is $S_0 = 1.29$
GPa for a gauge length $L_0 = 1$ m at 600°C. The interface sliding stress τ_0 is sensitive to
temperature, decreasing from about 120 MPa at ambient temperature to about 20 MPa at
600°C. The value of $\tau_0 = 20$ MPa at 600°C is used in the calculations. Using eqn (2b), we
find the characteristics stress for this fibrous system to be $S_c = 3.36$ GPa at 600°C. The
critical value of the damage parameter used in the calculation is $\omega_{cr} = 0.99$.

Plane stress conditions are assumed, and a constant tensile stress of $\sigma_{app} = 250$ MPa is
applied in the direction of the fibers. The load is increased linearly with time to its final
value of 250 MPa in 20 seconds and is then kept constant. Again, due to the symmetries of
the structure and the applied loads, we only consider a quarter of the plate. Four-node
isoparametric elements with 2×2 Gauss integrations are used in the calculations.

Figure 2 shows the variations of the axial stress σ_{22}, the axial strain ε_{22}, and the damage
parameter ω ahead of the hole along the x_1-axis at time $t = 20$ seconds, 1, 5, and 8 hours.
The stress concentration factor at the root of the hole just after the load is fully applied
($t = 20$ s) is about 3.5, corresponding to a local tensile stress of about 875 MPa. The value
of the damage parameter ω at the root of the hole is about 0.10 at that instant. As discussed
in the Appendix, the elastic strength of the composite is about 1090 MPa. The damage
parameter ω increases with time at the root of the hole and eventually causes local failure.
The curves shown in Fig. 2 make it clear that a crack like defect is formed at the root of
the hole and propagates along the x_1-axis. The stress is relaxed in the fully damaged region
due to fiber unloading; the small non-zero value of stress carried by the damaged region as
shown in Fig. 2a, is due to the fact that the damage parameter is not let to grow beyond
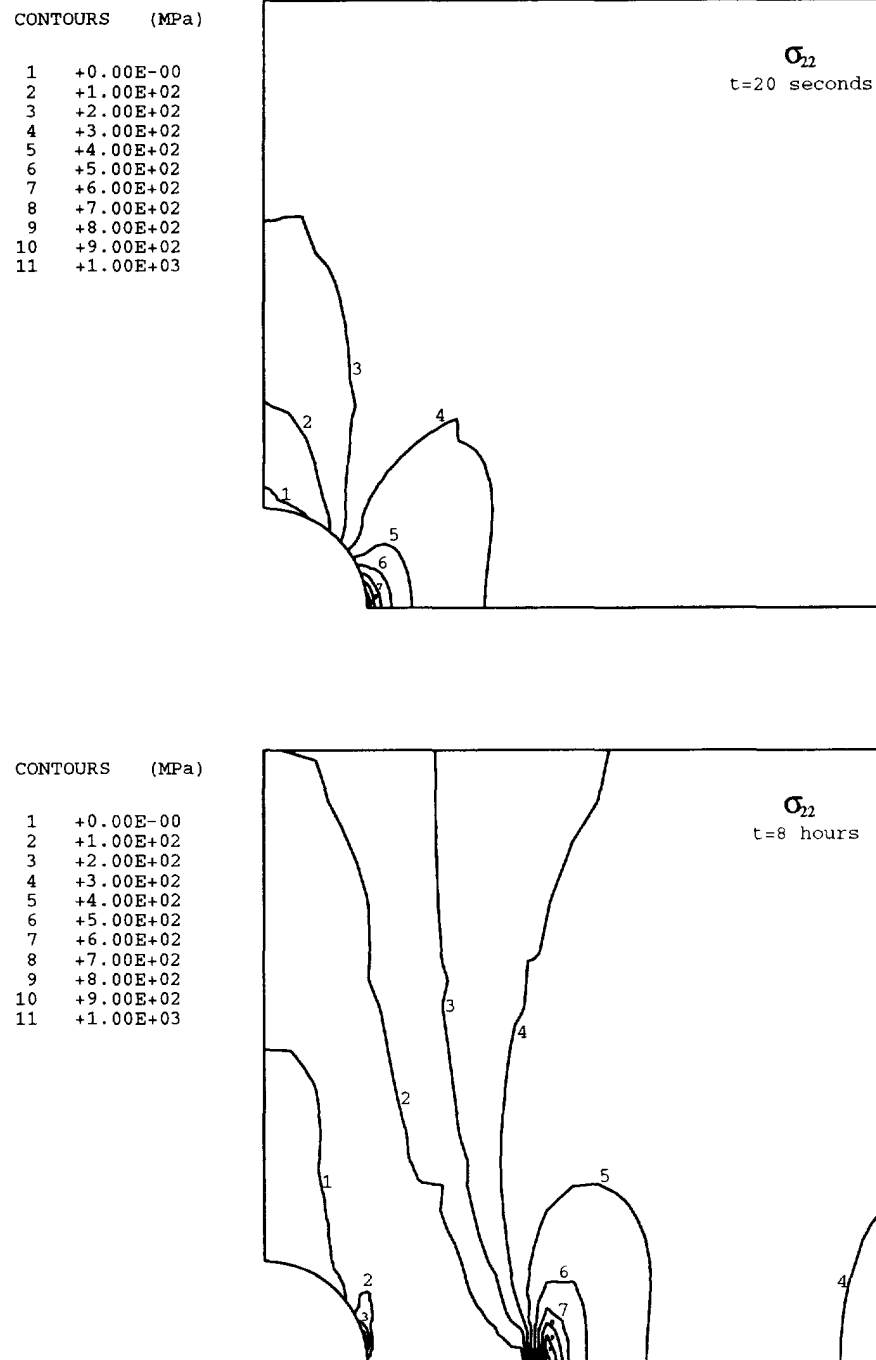the critical value of $\omega_{cr} = 0.99$.

CONTOURS   (MPa)

1	+0.00E-00
2	+1.00E+02
3	+2.00E+02
4	+3.00E+02
5	+4.00E+02
6	+5.00E+02
7	+6.00E+02
8	+7.00E+02
9	+8.00E+02
10	+9.00E+02
11	+1.00E+03

σ_{22}
t=20 seconds

CONTOURS   (MPa)

1	+0.00E-00
2	+1.00E+02
3	+2.00E+02
4	+3.00E+02
5	+4.00E+02
6	+5.00E+02
7	+6.00E+02
8	+7.00E+02
9	+8.00E+02
10	+9.00E+02
11	+1.00E+03

σ_{22}
t=8 hours

Fig. 3. Contours of the axial stress σ_{22} at time $t = 20$ sec and 8 hours.

CONTOURS

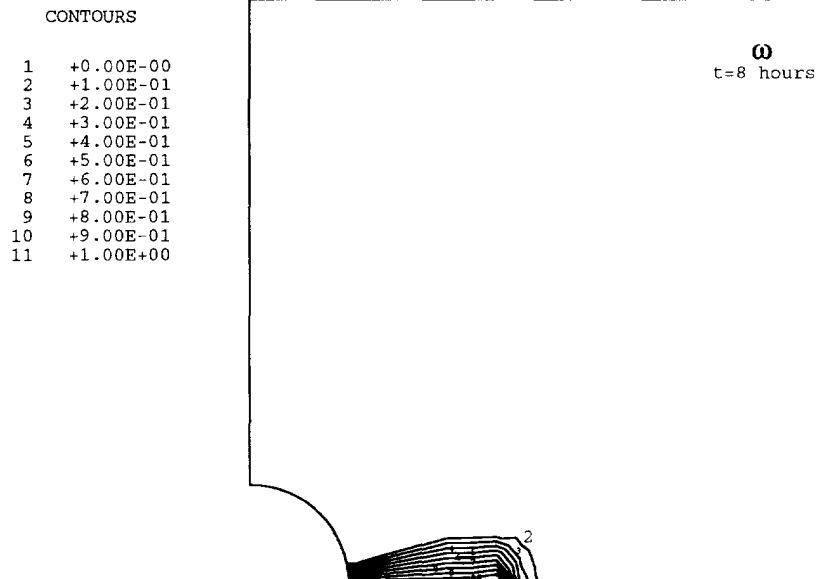| 1	+0.00E-00
2	+1.00E-01
3	+2.00E-01
4	+3.00E-01
5	+4.00E-01
6	+5.00E-01
7	+6.00E-01
8	+7.00E-01
9	+8.00E-01
10	+9.00E-01
11	+1.00E+00

ω
$t=8$ hours

Fig. 4. Contours of the damage parameter ω at time $t = 8$ hours.

Figure 3 shows contours of the axial stress at time $t = 20$ seconds and 8 hours. The stress concentration moves with the 'crack tip' of the aforementioned defect. Figure 4 shows contours of the damage parameter ω at time $t = 8$ hours. The extent of 'crack propagation' is evident in that figure.

REFERENCES

Aravas, N., Cheng, C. and Ponte Castañeda, P. (1995) Steady state creep of fiber-reinforced composites: constitutive equations and computational issues. *International Journal of Solids and Structures* **32**, 2218–2244.

Cheng, C. (1996) Creep of fiber-reinforced metal-matrix composites. Ph.D. thesis, Department of Mechanical Engineering and Applied Mechanics, University of Pennsylvania.

Christensen, R. M. (1979) *Mechanics of Composite Material.* Wiley, New York.

Curtin, W. A. (1991) Theory of mechanical properties of ceramic matrix composites. *Journal of the American Ceramic Society* **74**, 2837.

Du, Z.-Z. and McMeeking, R. M. (1995) Creep models for metal-matrix composites with long brittle fibers. *Journal of the Mechanics and Physics of Solids* **43**, 701–726.

Hibbitt, H. D. (1984) ABAQUS/EPGEN—A general purpose finite element code with emphasis on nonlinear applications. *Nuclear Engineering Design* **77**, 271–297.

Hild, F., Larsson, P.-L. and Leckie, F. A. (1992) Localization due to damage in fiber-reinforced composites. *International Journal of Solids and Structures* **29**, 3221–3238.

Jansson, S., Deve, H. E. and Evans A. G. (1991) The anisotropic mechanical properties of a Ti matrix composite reinforced with SiC fibers. *Metalica Transactions* **22a**, 2975–2984.

McLean, M. (1985) Creep deformation of metal-matrix composites. *Composite Science Technology* **23**, 37–52.

McLean, M. (1988) Mechanisms and models of high temperature deformation of composites. *Materials Research Symposium Proceedings* **120**, 67–79.

McLean, M. (1989) Creep of metal-matrix composites. In *Materials and Engineering Design: The Next Decade*, ed B. F. Dyson and D. R. Hayhust, p. 287. Institute of Metals, London.

Prewo, K. (1986) Tension and flexural strength of silicon carbide fiber-reinforced glass ceramics. *Journal of Material Science* **21**, 3590–3600.

Thouless, M. D., Sbaizero, O., Sigl, L. S. and Evans, A. G. (1989) Effect of interface mechanical properties on pullout in a SiC-reinforced lithium aluminum silicate glass-ceramics. *Journal of the American Ceramic Society* **72**, 525–532.

Weber, C. H., Du, Z.-Z. and Zok, F. W. (1996) High temperature deformation and fracture of a fiber reinforced Titanium matrix composite. *Acta Metallica Materiala* **44**, 683–695.

APPENDIX: THE DAMAGE PARAMETER ω

The physical meaning of the damage parameter ω is discussed in this section. The response of the composite is assumed to be purely elastic, i.e., both the fibers and the matrix can deform only elastically. For simplicity, we consider uniaxial loading in the direction of the fibers with a monotonically increasing axial strain ε.

Using the McLean assumptions, we can write

$$\sigma = f\bar{\sigma}_f + (1-f)\sigma_m \quad \text{and} \quad \varepsilon = \frac{\bar{\sigma}_f}{E_f^{sec}} = \frac{\sigma_m}{E_m}. \tag{74}$$

Equations (74b) can be written as

$$\bar{\sigma}_f = \left[1 - \frac{1}{2}\left(\frac{E_f\varepsilon}{S_c}\right)^{m+1}\right]E_f\varepsilon \quad \text{and} \quad \sigma_m = E_m\varepsilon. \tag{75}$$

Using eqn (74a), we find that the uniaxial stress–strain relationship of the composite is given by

$$\sigma = \left[1 - \frac{fE_f}{2E}\left(\frac{E_f\varepsilon}{S_c}\right)^{m+1}\right]E\varepsilon, \tag{76}$$

where $E = fE_f + (1-f)E_m$. Recalling the definition of ω:

$$\omega = (m+2)\frac{fE_f}{2E}\left(\frac{E_f\varepsilon}{S_c}\right)^{m+1}, \tag{77}$$

we can readily show that

$$\sigma = \left(1 - \frac{\omega}{m+2}\right)E\varepsilon \quad \text{and} \quad \bar{\sigma}_f = \left(1 - \frac{E}{fE_f}\frac{\omega}{m+2}\right)E_f\varepsilon, \tag{78}$$

so that

$$\frac{\mathrm{d}\sigma}{\mathrm{d}\varepsilon} = (1-\omega)E \quad \text{and} \quad \frac{\mathrm{d}\bar{\sigma}_f}{\mathrm{d}\varepsilon} = \left(1 - \frac{E}{fE_f}\omega\right)E_f. \tag{79}$$

The σ–ε and $\bar{\sigma}_f$–ε curves have a maximum at

$$\omega = 1 \quad \text{and} \quad \omega = \frac{fE_f}{E} < 1, \tag{80}$$

respectively. The corresponding maximum stress values are

$$\sigma_{max} = \frac{m+1}{m+2}\left(\frac{2}{m+2}\frac{E}{fE_f}\right)^{1/(m+1)}\frac{E}{E_f}S_c, \quad \text{and} \quad \bar{\sigma}_{fmax} = \frac{m+1}{m+2}\left(\frac{2}{m+2}\right)^{1/(m-1)}S_c, \tag{81}$$

and occur at strains

$$\varepsilon_{max} = \left(\frac{2}{m+2}\frac{E}{fE_f}\right)^{1/(m-1)}\frac{S_c}{E_f}, \quad \text{and} \quad \varepsilon_{fmax} = \left(\frac{2}{m+2}\right)^{1/(m+1)}\frac{S_c}{E_f} < \varepsilon_{max}, \tag{82}$$

respectively.

Equation (80a) makes it clear that, when the response of the composite is purely elastic. the value $\omega = 1$ coincides with the point of instability on the σ–ε curve.

Figure 5 shows the variations of σ, $\alpha = f\bar{\sigma}_f$, σ_m, and ω with strain ε, for $E_f/E_m = 360/65$, $f = 0.32$, and $m = 5$; the points of maximum stress are marked on the σ and α curves.

For the material system used in the finite element calculations on Section 5 ($E = 360$ GPa, $E_m = 65$ GPa, $f = 0.32$, $m = 5$, $S_0 = 1.29$ GPa, $L_0 = 1$ m, $\tau_0 = 20$ MPa, $D = 100$ μm), we have $S_c = 3.36$ GPa, and the maximum stresses

$$\sigma_{max} = 1.09\,\text{GPa} \quad \text{and} \quad \bar{\sigma}_{fmax} = 2.34\,\text{GPa}, \tag{83}$$

occur at

$$\varepsilon_{max} = 0.0080 \quad \text{and} \quad \varepsilon_{fmax} = 0.0076, \tag{84}$$
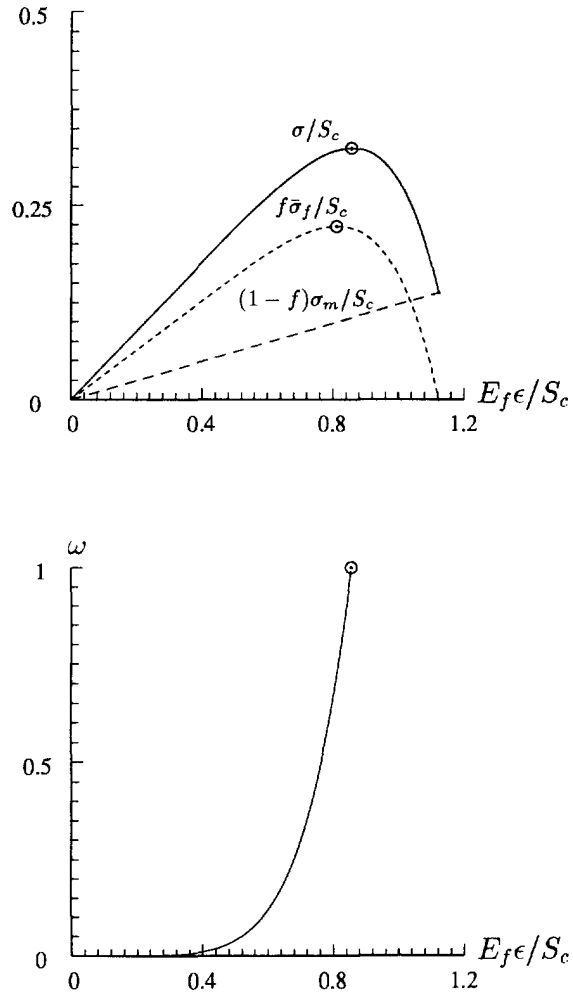
respectively.

Fig. 5. Variations of stresses σ, $\alpha = f\bar{\sigma}_f$, σ_m, and the damage parameter ω with strain ε, for $E_f/E_m = 360/65$, $f = 0.32$, and $m = 5$.